J Therm Anal Calorim (2011) 105:831–836
DOI 10.1007/s10973-010-1233-7

Synthesis, characterization and thermal behaviour of light trivalent lanthanides folates on solid state

P. R. Dametto · F. J. Caires · B. Ambrozini · M. Ionashiro

ESTAC2010 Conference Special Issue

Abstract Solid state Ln_2–L_3 compounds, where Ln stands for light trivalent lanthanides (lanthanum to gadolinium), except promethium, and L is folate ($C_{19}H_{17}N_7O_6$), have been synthesized. Simultaneous thermogravimetry and differential thermal analysis (TG-DTA), differential scanning calorimetry (DSC), X-ray powder diffractometry, infrared spectroscopy (FTIR), TG coupled to FTIR, elemental analysis and complexometry were used to characterize and to study the thermal behaviour of these compounds. The results provided information concerning the stoichiometry, crystallinity, ligand's denticity, thermal stability, thermal behaviour and identification of the gaseous products evolved during the thermal decomposition of these compounds.

Keywords Light lanthanides · Folate · Characterization · Thermal behaviour

Introduction

Folic acid is a member of Vitamin-B family that is necessary to healthy function of a variety of bodily processes. Folic acid and its derivatives are widespread in the nature. Folic acid is a specific growth factor for certain micro-organisms; however, in animals, the intestinal bacteria provide small amount needed for growth. It acts as co-enzyme in the normal DNA synthesis and also functions as part of the co-enzyme system in amino acid and nucleoprotein synthesis [1]. The structural diversity found in metal folate complexes could be attributed to the versatile behaviour of the folate anion, which may to act as bidentate, bridging bidentate or as a monodentate ligand [2–4].

A survey of the literature shows that the thermal studies involving folic acid or its compounds with metal ions is lacking. The articles published are concerned with Thermal stability of folic acid in the solid state [1], Synthesis, spectroscopic and thermal characterization of some transition metal complexes of folic acid [4] and Processes to identify the degradation mechanism of a solid which appears to undergo a complex reaction: folic acid [5].

In this article, the object of the present research was to prepare solid state compounds of light trivalent lanthanides (i.e. La to Gd, except Pm) with folate and to investigate by means of complexometry, elemental analysis, X-ray powder diffractometry, infrared spectroscopy (FTIR), simultaneous thermogravimetry and differential thermal analysis (TG-DTA), differential scanning calorimetry (DSC) and TG coupled to FTIR.

Experimental

The folic acid ($C_{19}H_{19}N_7O_6$) with 99% purity was obtained from Aldrich. Aqueous solution of Na_2–$C_{19}H_{17}N_7O_6$ 0.1 mol dm^{-3} was prepared from aqueous ($C_{19}H_{19}N_7O_6$) suspension by adding sodium hydroxide solution 2.5 mol dm^{-3} up to near total neutralization, followed by NaOH solution 0.1 mol dm^{-3} up to pH 8.0.

Lanthanide chlorides were prepared from the corresponding metal oxides (except for cerium) by treatment with hydrochloric acid solution. The resulting solutions were evaporated to near dryness, the residues were again dissolved in distilled water, transferred to a volumetric flask and diluted in order to obtain ca. 0.1 mol dm^{-3} solution,

---

P. R. Dametto (✉) · F. J. Caires · B. Ambrozini · M. Ionashiro
Instituto de Química, UNESP, C.P. 355, Araraquara,
SP CEP 14801-970, Brazil
e-mail: pdametto@gmail.com

Table 1 Analytical data for $Ln_2(L)_3\cdot nH_2O$

Compound	Water/%		Ligand lost/%		Metal oxide/%			Carbon/%		Hydrogen/%		Residue
	Calcd.	TG	Calcd.	TG	Calcd.	TG	EDTA	Calcd.	E.A.	Calcd.	EA	
$La_2(L)_3\cdot 9.5H_2O$	9.69	9.74	71.88	72.42	18.43	17.84	18.35	38.74	39.02	4.00	4.03	La_2O_3
$Ce_2(L)_3\cdot 6H_2O$	6.34	6.17	73.45	73.37	20.21	20.46	20.22	40.12	40.08	3.73	3.72	CeO_2
$Pr_2(L)_3\cdot 8H_2O$	8.27	8.40	72.24	71.90	19.49	19.69	20.07	39.25	39.07	3.88	3.87	Pr_6O_{11}
$Nd_2(L)_3\cdot 6.5H_2O$	6.80	7.04	73.73	73.14	19.47	19.82	19.76	39.71	39.39	3.75	3.73	Nd_2O_3
$Sm_2(L)_3\cdot 8H_2O$	8.18	8.11	72.03	72.17	19.79	19.71	19.80	38.83	38.91	3.84	3.84	Sm_2O_3
$Eu_2(L)_3\cdot 9H_2O$	9.09	8.92	71.15	71.27	19.76	19.81	20.28	38.37	38.43	3.91	3.91	Eu_2O_3
$Gd_2(L)_3\cdot 9H_2O$	9.04	8.99	70.75	71.61	20.21	19.39	20.27	38.14	38.60	3.88	3.92	Gd_2O_3

Ln La(III), Ce(III), Pr(III), Nd(III), Sm(III), Eu(III), Gd(III); *L* Folate

Table 2 Spectroscopic data for sodium folate and compounds with lighter trivalent lanthanides

Compound	$\nu_{as(COO^-)}/cm^{-1}$	$\nu_{s(COO^-)}/cm^{-1}$	$\Delta\nu(\nu_{as} - \nu_s)/cm^{-1}$
Na_2L	1564_s	1392_s	172
$La_2(L)_3\cdot 9.5H_2O$	1503_s	1402_s	101
$Ce_2(L)_3\cdot 6H_2O$	1502_s	1402_s	100
$Pr_2(L)_3\cdot 8H_2O$	1503_s	1402_s	101
$Nd_2(L)_3\cdot 6.5H_2O$	1506_s	1404_s	102
$Sm_2(L)_3\cdot 8H_2O$	1505_s	1403_s	102
$Eu_2(L)_3\cdot 9H_2O$	1503_s	1402_s	101
$Gd_2(L)_3\cdot 9H_2O$	1495_s	1392_s	103

s strong, *L* folate

$\nu_{s(COO^-)}$ and $\nu_{as(COO^-)}$ symmetrical and anti-symmetrical vibrations of the COO^- structure

Fig. 1 TG-DTA curves of: **a** $La_2(L)_3\cdot 9.5H_2O$ ($m = 7.126$ mg); **b** $Ce_2(L)_3\cdot 6H_2O$ ($m = 7.045$ mg); **c** $Pr_2(L)_3\cdot 8H_2O$ ($m = 6.962$ mg); **d** $Nd_2(L)_3\cdot 6.5H_2O$ ($m = 7.230$ mg); **e** $Sm_2(L)_3\cdot 8H_2O$ ($m = 7.243$ mg); **f** $Eu_2(L)_3\cdot 9H_2O$ ($m = 7.237$ mg); **g** $Gd_2(L)_3\cdot 9H_2O$ ($m = 7.408$ mg). *L* folate

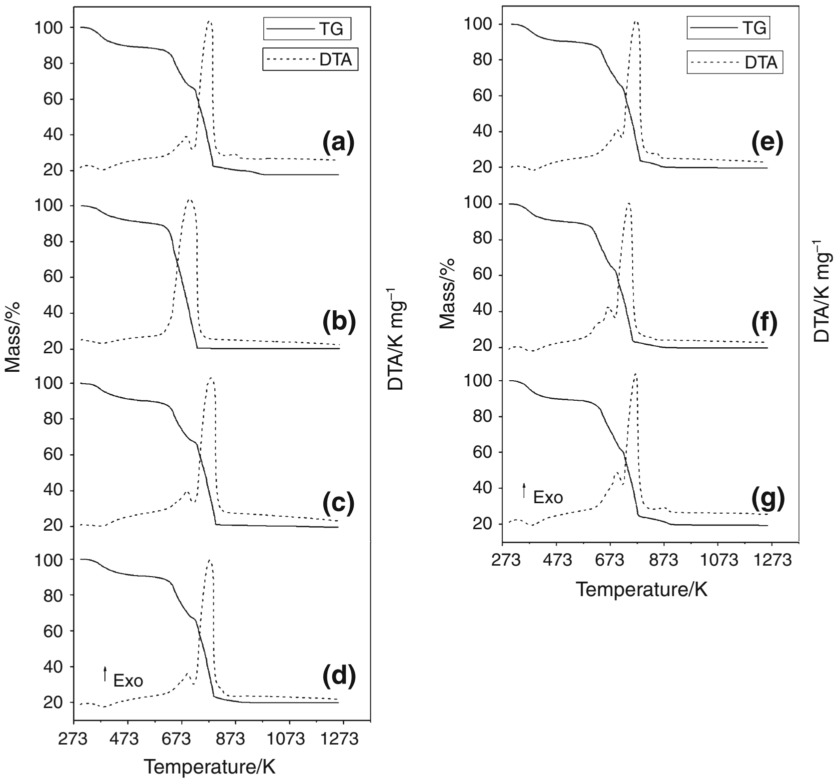

Table 3 Temperature ranges (*T*), mass losses (%), and peak temperature observed for each step of the TG-DTA curves of the compounds $Ln_2(L)_3 \cdot nH_2O$ where Ln = trivalent lanthanides and L = folate

Compound	Steps			
	First	Second	Third	Fourth
$La_2(L)_3 \cdot 9.5H_2O$				
T/K	303–448	448–724	724–793	793–1008
Loss/%	9.74	24.48	43.25	4.69
Peak/K	382	693	783	873
$Ce_2(L)_3 \cdot 6H_2O$				
T/K	303–418	418–723	–	–
Loss/%	6.17	73.37	–	–
Peak/K	376	703	–	–
$Pr_2(L)_3 \cdot 8H_2O$				
T/K	303–458	458–718	718–813	–
Loss/%	8.40	25.85	46.05	–
Peak/K	374	693	773	–
$Nd_2(L)_3 \cdot 6.5H_2O$				
T/K	303–423	423–733	733–798	798–903
Loss/%	7.04	26.82	43.07	3.25
Peak/K	385	698	783	sh 823
$Sm_2(L)_3 \cdot 8H_2O$				
T/K	303–428	428–721	721–788	788–883
Loss/%	8.11	25.12	43.51	3.54
Peak/K	383	698	773	848
$Eu_2(L)_3 \cdot 9H_2O$				
T/K	303–443	443–691	691–758	758–898
Loss/%	8.92	26.55	41.22	3.50
Peak/K	381	663	748	823
$Gd_2(L)_3 \cdot 9H_2O$				
T/K	303–423	423–723	723–773	773–913
Loss/%	8.99	30.58	35.40	5.63
Peak/K	379	698	763	878

sh Shoulder

whose pH were adjusted to 5.0 by adding diluted sodium hydroxide or hydrochloric acid solutions. Cerium(III) was used as its nitrate and ca 0.1 mol dm^{-3} aqueous solution of this ion was prepared by direct weighing of the salt.

The solid state compounds were prepared by adding slowly, with continuous stirring, the aqueous solution of the Na_2–$C_{19}H_{17}N_7O_6$ to the respective metal chloride until total precipitation of the metal ions. The precipitates were washed with distilled water until elimination of chloride ions (qualitative test with $AgNO_3/HNO_3$ solution to chloride ions or diphenylamine solution to nitrate ions), filtered through and dried on Whatman no. 42 filter paper and kept in a desiccator over anhydrous calcium chloride.

In the solid state compounds, hydration water, ligand and metal ion content were determined from TG curves. The metal ions were also determined by complexometric titrations with standard EDTA solution using xylenol orange as indicator after igniting the compounds to the respective oxides and their dissolution in hydrochloric acid [6].

X-ray powder patterns were obtained by using a SIEMENS D-5000 X-ray diffractometer employing Cu K_α radiation ($\lambda = 1.541$ Å) and setting of 40 kV and 20 mA.

The attenuate total reflectance infrared spectra for sodium folate and for its metal-ion compounds were run on a Nicolet iS10 FT-IR spectrophotometer, using an ATR accessory with Ge window.

Carbon and hydrogen contents were determined by microanalytical procedures, with a CHN Elemental Analyser from Perkin Elmer, model 2400.

Simultaneous TG-DTA curves and DSC curves were obtained with two thermal analysis systems, models SDT 2960 and Q10 both from TA Instruments, respectively. The purge gas was an air flow of 100 cm^3 min^{-1} (TG-DTA) and 50 cm^3 min^{-1} (DSC). A heating rate of 20 K min^{-1} and with samples weighing about 7 mg (TG-DTA) and about 5 mg (DSC). Alumina and aluminium crucibles, the latter with perforated cover, were used for TG-DTA and DSC, respectively.

The measurements of the gaseous products were carried out using a Thermogravimetric Analyzer Mettler TG-DTA coupled to a FTIR spectrophotometer Nicolet with gas cell and DTGS KBr detector. The furnace and the heated gas cell (523 K) were coupled through a heated ($T = 473$ K) 120-cm stainless steel line transfer with diameter of 2 mm, both purged with dry air (50 cm^3 min^{-1}). The FTIR spectra were recorded with 32 scans per spectrum at a resolution of 4 cm^{-1}.

Results and discussion

The analytical, thermoanalytical (TG) and elemental analysis results are shown in Table 1. These results establish the stoichiometry of these compounds, which are in agreement with the general formula, $Ln_2(C_{19}H_{17}N_7O_6)_3 \cdot nH_2O$, where Ln represents La(III), Ce(III), Pr(III), Nd(III), Sm(III), Eu(III) or Gd(III), $C_{19}H_{17}N_7O_6$ is folate and $n = 9.5$ (La), 6.0 (Ce), 8.0 (Pr), 6.5 (Nd), 8.0 (Sm), 9.0 (Eu) and 9.0 (Gd).

X-ray powder patterns showed that all the compounds were obtained in amorphous state. The amorphous states undoubtedly related to the low solubility of these compounds.

Infrared spectroscopic data on sodium folate (Na_2–$C_{19}H_{17}N_7O_6$) and its compounds with the metal ions considered in this study are shown in Table 2. The investigation was focused mainly within the 1700–1400 cm^{-1}

Fig. 2 DSC curves of:
a $La_2(L)_3{\cdot}9.5H_2O$;
b $Ce_2(L)_3{\cdot}6H_2O$;
c $Pr_2(L)_3{\cdot}8H_2O$;
d $Nd_2(L)_3{\cdot}6.5H_2O$;
e $Sm_2(L)_3{\cdot}8H_2O$;
f $Eu_2(L)_3{\cdot}9H_2O$;
g $Gd_2(L)_3{\cdot}9H_2O$. *L* folate

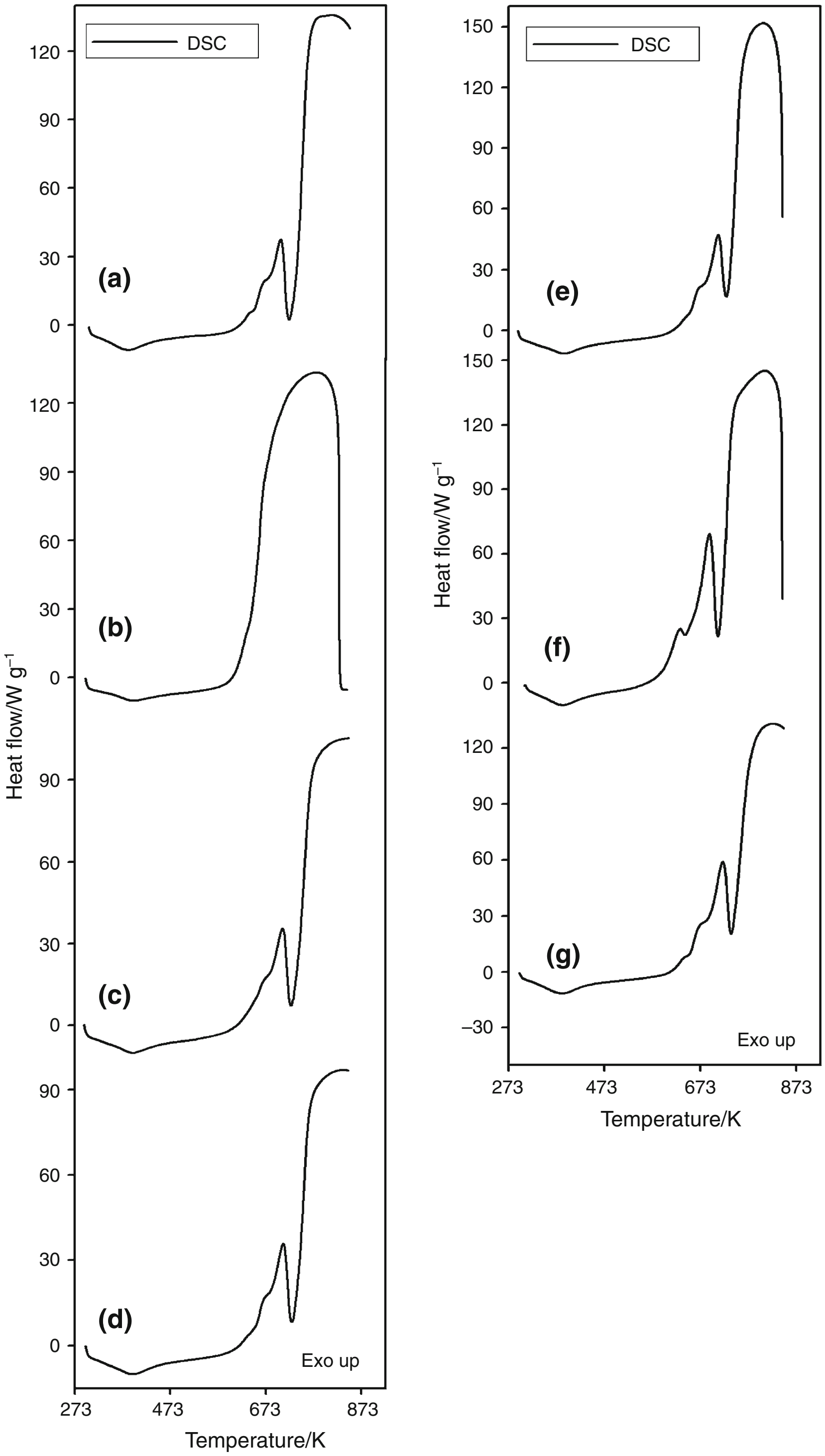

range because the region is potentially most informative in attempting to assign coordination sites. In the Na_2–$C_{19}H_{17}N_7O_6$, strong bands located at 1564 and 1392 cm^{-1} are attributed to anti-symmetrical (ν_{as}) and symmetrical (ν_{sym}) frequencies of the carboxylate groups, respectively [7, 8]. For the synthesized compounds, the band assigned to the anti-symmetrical stretching carboxylate frequencies are shifted to lower values and the symmetrical ones to higher, relative to the corresponding frequencies in $C_{19}H_{17}N_7O_6$. The $\Delta\nu$ ($\nu_{as} - \nu_s$) for these compounds is indicative that these lanthanides are linked to the carboxylate group by a bridging bond [9].

Simultaneous TG-DTA curves of the compounds are shown in Fig. 1. These curves exhibit mass losses in two

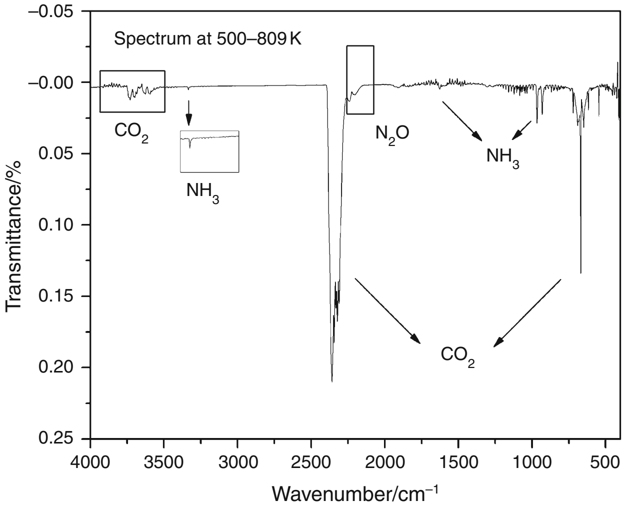

Fig. 3 IR spectrum of gaseous products evolved during the decomposition of the samarium folate between 500 and 809 K

(Ce), three (Pr) or four (La, Nd, Sm, Eu, Gd) steps between 303 and 1008 K. The first mass loss between 303 and 453 K (La–Gd), corresponding to the endothermic peak at 382 K (La), 376 K (Ce), 374 K (Pr), 385 K (Nd), 383 K (Sm), 381 K (Eu) and 379 K (Gd) is due to dehydration, which occurs in a single step.

After dehydration, the mass losses observed above 448 K (La), 418 K (Ce), 458 K (Pr), 423 K (Nd), 428 K (Sm), 443 K (Eu) and 423 K (Gd) are due to the thermal decomposition of the anhydrous compounds; these take place in consecutive and/or overlapping steps with partial losses which are characteristic for each compound.

For the anhydrous cerium compound, the thermal decomposition occurs in a single step up to 723 K with the formation of cerium(IV) oxide CeO_2, as final residue. The smaller final temperature of thermal decomposition is due to the oxidation reaction of Ce(III) to Ce(IV), together with the oxidation of the organic matter. This behaviour had already been observed for other cerium compounds [10–12].

For the other anhydrous compounds, the mass loss up to 1008 K (La), 813 K (Pr), 903 K (Nd), 883 K (Sm), 898 K (Eu) and 913 K (Gd) corresponding to endothermic or exothermic peaks are attributed to the thermal decomposition being the exothermic events due to the oxidation of the organic matter (Fig. 1). Calculations based on the total mass losses observed in the TG curves are in agreement with the formation of the respective oxides, Pr_6O_{11}, Ln_2O_3 (L = La, Nd, Sm, Eu, Gd). The mass losses, temperature ranges and the peak temperatures observed in each step of the TG-DTA curves are shown in Table 3.

The DSC curves of the compounds are shown in Fig. 2. These curves show endothermic and exothermic peaks that all are in agreement with the mass losses observed in the TG curves. The endothermic peak at 380–395 K is assigned to the dehydration, which occurs in single step. The dehydration enthalpies found for the compounds (La to Gd) were: 60.05, 61.17, 85.86, 107.07, 121.39, 163.10 and 193.55 kJ mol^{-1}, respectively.

The gaseous products evolved during the thermal decomposition of the compounds studied in this work were monitored by FTIR. The TG-DTA curve and IR spectrum of the gaseous products evolved during the thermal decomposition of samarium folate, as representative of all the compounds is shown in Fig. 3. The monitoring of evolved gases during the thermal decomposition was: ammonia, nitric oxide and carbon dioxide due to descarboxylation and oxidation of organic matter.

Conclusions

From analytical and thermoanalytical (TG) results, a general formula could be established for these compounds in the solid state.

The X-ray powder patterns showed that all the compounds synthesized showed low crystallinity degree.

The infrared spectroscopic data suggest that the $C_{19}H_{17}N_7O_6$ acts as a bridging ligand towards the metal ions considered in this work.

The TG-DTA and DSC curves provided information about the thermal stability and thermal behaviour of these compounds.

Acknowledgements The authors thank FAPESP, CNPq and CAPES Foundations (Brazil) for financial support.

References

1. Vora A, Riga A, Dollimore D, Alexander K. Thermal stability of folic acid in the solid-state. J Therm Anal Calorim. 2004;75:709–17.
2. Mehrotra RC, Bohra R. Metal carboxylates. London: Academic Press; 1983.
3. Mehrotra RC, Singh A. Recent trends in metal alkoxide chemistry. Prog Inorg Chem. 1997;46:239–454.
4. Abd El-Wahed MG, Refat MS, El-Megharbel SM. Synthesis, spectroscopic and thermal characterization of some transition metal complexes of folic acid. Spectrochim Acta A. 2008;70:916–22.
5. Vora A, Riga A, Alexander K. Processes to identify the degradation mechanism of a solid which appears to undergo a complex reaction: folic acid. Instrum Sci Technol. 2002;30:193–203.
6. Ionashiro M, Graner CAF, Zuanon Netto J. Titulação complexométrica de lantanídeos e ítrio. Ecl Quim. 1983;8:29–32.
7. Sócrates G. Infrared characteristic group frequencies. 2nd ed. New York: Wiley; 1994.
8. Silverstein RM, Webster FX. Spectrometric identification of organic compounds. 6th ed. New York: Wiley; 1998.

9. Deacon GB, Phillips RJ. Relationships between the carbon-oxygen stretching frequencies of carboxylate complexes and the type of carboxylate coordination. Coord Chem Rev. 1980;33:227–50.
10. Dametto PR, Siqueira AB, Carvalho CT, Ionashiro M. Synthesis, characterization and thermal studies on solid state 3-methoxybenzoate of lighter trivalent lanthanides. Ecl Quim. 2007;32: 17–21.
11. Siqueira AB, Bannach G, Rodrigues EC, Carvalho CT, Ionashiro M. Solid-state 2-methoxybenzoates of light trivalent lanthanides: synthesis, characterization and thermal behaviour. J Therm Anal Calorim. 2008;91:897–902.
12. Ambrozini B, Dametto PR, Siqueira AB, Carvalho CT, Ionashiro M. Synthesis, characterization and thermal behavior on solid tartrates of light trivalent lanthanides. J Therm Anal Calorim. 2009;97:761–4.